

Magnetic-field antisymmetry of photovoltaic voltage in evanescent microwave fields as seen in a semiconductor Hall bar

A. Chepelianskii,¹ S. Guéron,¹ F. Pierre,² A. Cavanna,² B. Etienne,² and H. Bouchiat¹

¹CNRS, UMR 8502, Université Paris-Sud, F-91405 Orsay, France

²Laboratoire de Photonique et de Nanostructures (LPN), CNRS, route de Nozay, 91460 Marcoussis, France

(Received 6 February 2009; published 7 May 2009)

A two-dimensional electron system without spatial inversion symmetry develops a sample specific dc voltage when exposed to a microwave radiation at low temperature. We investigate this photovoltaic (PV) effect in the case where spatial symmetry is broken by an evanescent high-frequency potential. We measure the induced PV voltage in a GaAs/Ga_{1-x}Al_xAs Hall bar at magnetic fields in the tesla range. We find that in this regime the induced PV voltage is antisymmetric with magnetic field and exhibits regular Shubnikov-de Haas-type oscillations. Our experimental results can be understood from a simple model, which describes the effect of stationary orbital currents caused by microwave driving.

DOI: 10.1103/PhysRevB.79.195309

PACS number(s): 73.50.Pz, 05.70.Ln, 72.20.My

I. INTRODUCTION

Coherent mesoscopic samples present remarkable rectification properties, related to the absence of spatial inversion symmetry of the disorder potential. In particular, when submitted to a radio-frequency radiation, they develop a dc voltage. The dependence on magnetic field of this photovoltaic (PV) effect gives rise to random but reproducible fluctuations that were predicted theoretically^{1,2} and observed experimentally in references.^{3,4} In contrast to the universal conductance fluctuations that obey Onsager symmetry rules,^{5,6} the fluctuations of the PV voltage do not have a well-defined magnetic-field symmetry.⁷ At high frequency this can be understood from the violation of time inversion symmetry by the microwave radiation.⁸⁻¹⁰ At low frequencies, this behavior was explained through a mechanism involving electron-electron interactions.¹¹⁻¹⁶ Recently the PV effect was studied in asymmetric antidot super lattices where magnetic-field asymmetry was also present.^{17,18} In all these cases, however, the antisymmetric component of the PV voltage was never larger than the symmetric one (see, e.g., Ref. 19). In this paper, we investigate the regime where the spatial symmetry of the system is broken by a nonhomogeneous high-frequency potential. This potential is screened in the region of the sample where the photovoltaic voltage is measured by a copper shield evaporated on the surface of the Hall bar. This reduces the mesoscopic fluctuations of the PV voltage, revealing a PV voltage with a dominant antisymmetric contribution.

II. PHOTOVOLTAIC VOLTAGE IN EVANESCENT MICROWAVE FIELDS

The system consists of a Hall bar in a GaAs/Ga_{1-x}Al_xAs two-dimensional electron gas (2DEG) with density $n_e \approx 1.2 \times 10^{11} \text{ cm}^{-2}$ and mobility $\mu \approx 1.1 \times 10^2 \text{ m}^2/\text{Vs}$. The sample was fabricated using wet etching and an aluminum mask. The six contacts of the Hall bar are numbered (1)–(6) (see photograph inset in Fig. 1). The four terminal resistances with source (i) and drain (j) and voltage probes k and l are defined by the usual relation $R_{ij,kl} = (V_k - V_l) / I_i$ where V_k and V_l are the voltages on the leads (k) and (l) and $I_i = -I_j$ is the

current injected in the source lead. We measure simultaneously the Hall resistances $R_{H,1} = R_{14,26}$, $R_{H,2} = R_{14,35}$, and the longitudinal resistance $R_{xx} = R_{14,23}$ as a function of magnetic-field H . As shown in Fig. 1 our samples exhibit quantum-Hall-effect plateaux²⁰ for the Hall resistances $R_{H,1}$, $R_{H,2}$ and Shubnikov-de Haas (SdH) oscillations²¹ in the transverse resistance R_{xx} . We notice that the carrier density in our system is homogeneous since $R_{H,1} \approx R_{H,2}$.

In the following, we excite the system with a high-frequency potential $V_{ac} \cos(2\pi ft)$ applied on a symmetrical split gate [S] shown in the inset of Fig. 1. This potential is screened by a 100-nm-thick copper top gate deposited over the Hall bar device and therefore the induced potential is spatially nonhomogeneous and vanishes exponentially inside the Hall bar.²² We note that while the topgate ensures a good

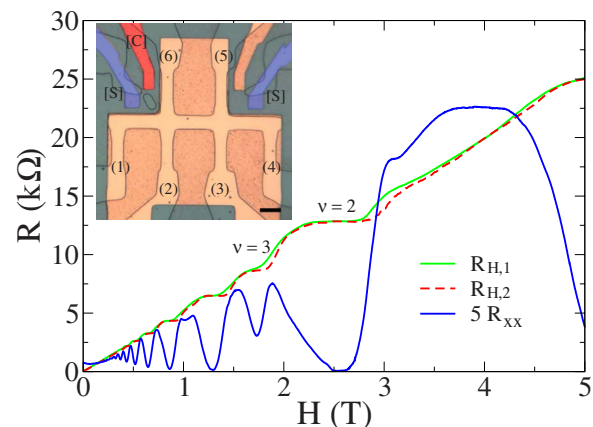


FIG. 1. (Color online) Magnetotransport properties of the Hall bar. The dashed and neighbor curves represent respectively the Hall resistances $R_{H,2} = R_{14,35}$ and $R_{H,1} = R_{14,26}$ (see text). The oscillating curve represents the longitudinal resistance $R_{xx} = R_{14,23}$. The data were acquired with a 100 nA excitation and lock-in detection at frequency 67 Hz at a temperature of 300 mK. The inset is an optical image of the sample, the leads (1)–(6) form the contacts of the Hall bar, while the electrodes [S] and [C] are local gates connected to a high-frequency 50 Ω transmission line. The (orange) copper shield on top of the Hall bar can be used as a top gate to change the carrier density in the 2DEG. The black scale bar corresponds to 10 μm .

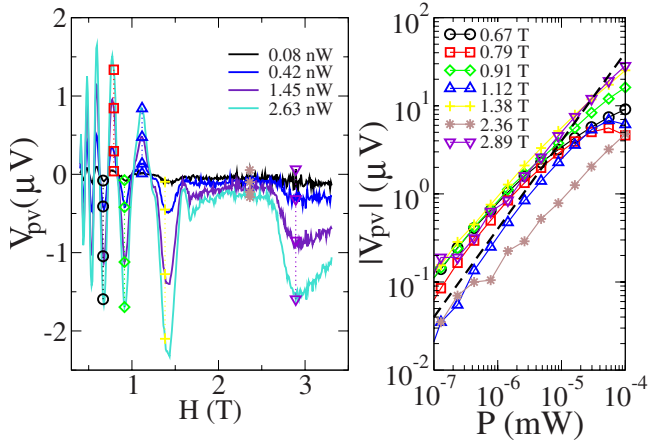


FIG. 2. (Color online) Left panel: magnetic-field dependence of the photovoltaic voltage V_{PV} for different microwave powers, namely, 0.08, 0.42, 1.45, and 2.63 nW in the direction of increasing oscillation amplitude. Right panel: dependence of the photovoltage amplitude V_{PV} as a function of microwave power for different values of the magnetic field (the symbols correspond to different magnetic fields and are indicated on both the right and left panels). The dashed line represents the dependence $V_{PV} \propto P$. Temperature is 300 mK, and frequency $f=2.5$ GHz.

shielding of the ac electric potential on the Hall probe, this is not the case for ac magnetic fields at frequencies below 10 GHz such that the skin depth is larger than 100 nm. However, we expect the effect of those fields to be negligible because of the electrostatic coupling between the rf lines and the Hall probe. We measure the PV voltage drop $V_{PV}=V_3 - V_2$ induced by the irradiation. In order to determine this voltage with a high precision, we modulate the high-frequency signal at a low frequency below 1.5 kHz. The voltage V_{PV} is then amplified by a low-noise amplifier and measured by a lock-in detector working at the frequency of the amplitude modulation. In Fig. 2, we have studied the dependence of V_{PV} on magnetic field and microwave power at fixed frequency $f=2.5$ GHz. The photovoltaic voltage displays oscillations as a function of magnetic-field reminiscent of SdH oscillations in the longitudinal resistance R_{xx} (Fig. 2, left panel), except that the PV voltage oscillates around a zero mean value which is not the case for the longitudinal resistance. We also notice that the oscillations of V_{PV} are quenched in the quantum-Hall plateau region around $H=2$ T (filling factor $\nu=2$), in contrast to oscillations in longitudinal resistance (see Fig. 1). The amplitude of these oscillations increases with the injected microwave power P . Since the microwaves are transmitted through a $Z_0=50 \Omega$ adapted line, P is related to the high-frequency potential amplitude through $V_{ac}^2 = \alpha Z_0 P$. Here α is a frequency-dependent coefficient taking into account the attenuation and reflection in the transmission line. We estimate that $\alpha \approx 0.1$ for frequencies in the gigahertz range. In the right panel of Fig. 2 we show the dependence of the rectified voltage on power more quantitatively at selected values of magnetic field. We find that the photovoltaic voltage is well described by $V_{PV} \propto P$, the deviations at higher power are attributed to heating effects. We have also performed experiments with asymmetric irradiation on the electrode [C], with the electrode oppo-

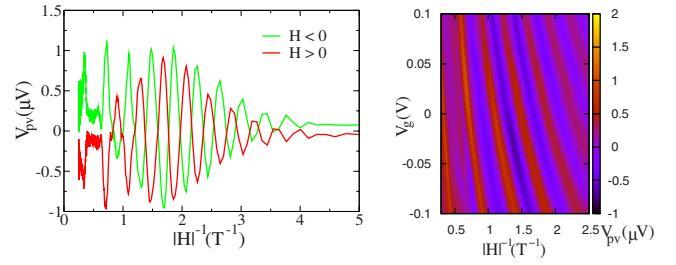


FIG. 3. (Color online) Left panel: comparison of the PV voltage V_{PV} as a function of inverse magnetic field for positive and negative magnetic fields. Frequency was $f=2.5$ GHz and injected microwave power of 1 nW. On the right panel, a color/grayscale diagram showing the PV voltage as a function of both top-gate voltage and applied magnetic field.

site to [C] floating. These experiments lead to a similar behavior with the difference that the oscillations of the PV voltage are no longer centered around zero. For this reason we focus on the case of symmetric irradiation on the local gate [S] in the rest of this paper.

III. MAGNETIC-FIELD ANTISYMMETRY

The SdH oscillations of resistivity in metals and in 2DEG are symmetric with magnetic field. In contrast as illustrated in the left panel of Fig. 3, we find that the oscillations of the photovoltage are mostly antisymmetric with magnetic field. In this figure, in order to make the connection with SdH oscillations more obvious, we have shown the photovoltage V_{PV} as a function of the inverse absolute value of the magnetic field. The photovoltage displays periodic oscillations with inverse magnetic field with the exception of a missing half period at $H^{-1} \approx 0.5 \text{ T}^{-1}$ in the quantum-Hall plateau regime (filling factor $\nu=2$). The right panel shows that the period of the oscillations of the photovoltage can be modified by changing the density n_e of the Hall probe with a top-gate voltage V_g . This further supports the connection with SdH oscillation of resistivity whose period τ_H is related to electron density through $\tau_H = e / (\pi \hbar n_e)$. We have also checked the antisymmetry of the photovoltage at different gate voltages. The data shown in Fig. 3 were obtained for $f=2.5$ GHz, at lower microwave frequencies, the photovoltage decreases and vanishes around $f \approx 10$ MHz while remaining mostly antisymmetric. We attribute this decrease in the inefficiency of our capacitive coupling at so low frequencies. We note that we are always in the regime $2\pi f < \omega_c$ where ω_c is the cyclotron frequency; therefore, we do not expect the frequency to play an important role in contrast to the recent experiments where a sharp frequency-dependent PV effect was investigated around $\omega = \omega_c$ (Ref. 23) in relation to the microwave-induced resistance oscillations and zero resistance states.^{24–26}

Under homogeneous irradiation, the photovoltage also displays $1/B$ oscillations with the period τ_H as shown in Fig. 4. However these oscillations contain a large symmetric component as a function of magnetic field in contrast to our data for evanescent irradiation. This is consistent with the previous experimental results reported in Refs. 8–10 where

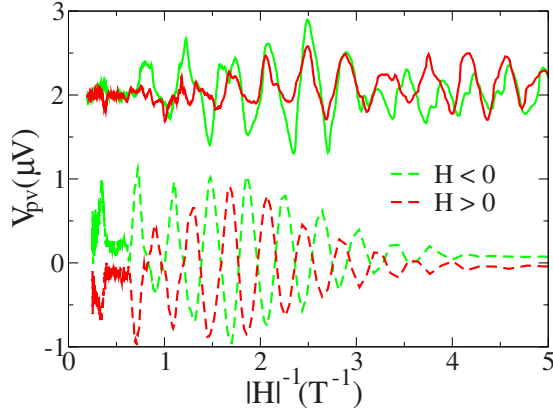


FIG. 4. (Color online) Comparison of the PV voltage V_{PV} as a function of inverse magnetic field for positive and negative magnetic fields. For the continuous curves microwave irradiation was sent using an external 3-mm-long antenna terminating a 50 Ω cryogenic coaxial cable. The dashed curves reproduce for comparison our data of Fig. 3 obtained by applying a high-frequency potential directly on the local split gate. In both cases frequency was $f = 2.5$ GHz. The continuous curves are shifted for clarity by 2 μV .

high-frequency photovoltaic effect did not exhibit a well-defined magnetic-field symmetry.

The SdH oscillations of longitudinal resistance R_{xx} as a function of inverse magnetic field have a well-defined phase, which is given by the expression $R_{xx}(H^{-1}) = R_0(H^{-1}) + R_1(H^{-1})\cos(\frac{2\pi^2 n_e \hbar}{eH})$, where $R_0(H^{-1})$ and $R_1(H^{-1})$ are envelope functions weakly depending on the magnetic field on the scale of one SdH oscillation period τ_H .²¹ In Fig. 5 (main figure) we compare the phase of the oscillations of V_{PV} and the phase of the oscillations in R_{xx} . Our results demonstrate that the oscillation of the photovoltage is dephased by $\pi/2$ compared to the oscillations of R_{xx} . We check this by calculating numerically the integral $\int V_{PV}(H^{-1})dH^{-1}$ from the experimental data. We find that oscillations of this quantity are

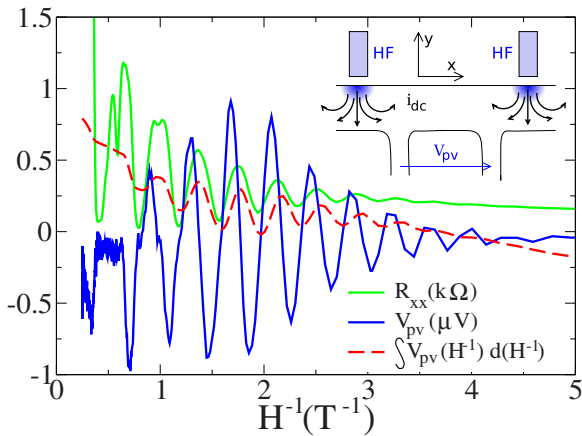


FIG. 5. (Color online) Comparison between the behavior of R_{xx} (k Ω) (green/gray curve), V_{PV} (μV) (blue/black curve), and $\int V_{PV}(H^{-1})dH^{-1}$ (red dashed curve). The inset shows a simplified sample geometry with schematic of induced stationary currents, i_{dc} , and density modulation (colored/grayscale semidisks). Frequency is $f = 2.5$ GHz and $P = 1$ nW.

in phase with the oscillations of $R_{xx}(H^{-1})$ (a theoretical argument justifying this comparison is given below).

In summary we find that the SdH oscillations of the PV voltage are antisymmetric with magnetic field and are out of phase with the usual SdH oscillation of resistivity as a function of H^{-1} . These oscillations are quenched in the plateau regions of the quantum-Hall effect. The main lines of our explanation are the following. The high-frequency potential applied on the local gate [5] creates a stationary current distribution i_{dc} inside the sample mostly along the y axis. A possible current distribution is shown in the inset of Fig. 5 with a simplified sample geometry. This current leads to the appearance of a static Hall voltage drop $V_{PV} \approx R_H i_{dc}$ along the x axis perpendicular to i_{dc} . For this expression to be valid, the applied potential V_{ac} must vanish in the region where V_{PV} is measured. Otherwise an additional contribution appears from mesoscopic fluctuations induced by the alternating potential. This contribution has a large symmetric component. In this respect, the evanescent potential geometry used in our experiment is crucial, and we have checked that under an homogeneous irradiation, we recover an essentially symmetric photovoltage.

IV. STATIONARY ORBITAL CURRENTS MODEL

It is possible to derive more quantitative estimates from this heuristic scenario. The potential V_{ac} on the local gate creates a modulation of the electronic density δn in the Hall bar. We assume that for high magnetic fields, this density modulation occurs in a region of typical Larmor radius $r_l = v_F m^* / eH$ inside the sample, where $v_F = \hbar \sqrt{2\pi n_e} / m^*$ is the Fermi velocity and m^* is the electron mass in 2DEG (colored regions in the sketch of Fig. 5). Indeed, in this regime, most electronic trajectories are localized on cyclotron orbits of radius r_l , which is, therefore, the natural length scale. The total charge induced on the Hall bar is given by CV_{ac} where C is the capacitance between the local gate and the Hall bar; hence, the amplitude of δn can be estimated as $\delta n \approx \frac{C}{r_l} V_{ac} \cos(2\pi ft)$. An approximate value of the capacitance is ϵD , where ϵ is the permittivity and D is the typical distance between the gate and the Hall bar. In the SdH regime, the amplitude of the rectified current i_{dc} is given by

$$i_{dc} \approx \left\langle \frac{\partial G_{yy}}{\partial n_e} \delta n V_{ac} \cos(2\pi ft) \right\rangle, \quad (1)$$

where $\langle \cdot \rangle$ denotes time averaging and G_{yy} is the conductance in the y direction of the sample. Up to a geometrical factor we have $G_{yy} \approx G_{xx}$ and in the regime where $R_{xx} \ll R_H$, G_{xx} is given by $G_{xx} \approx R_{xx} / R_H^2$. As noted above, $R_{xx} = R_0 + R_1 \cos(\frac{2\pi^2 n_e \hbar}{eH})$ where R_0 and R_1 are slow functions of density and inverse magnetic field. This allows us to take into account only the oscillating term in the density derivative, which yields

$$i_{dc} \approx \frac{\hbar}{eH} \frac{R_1 \sin\left(\frac{2\pi^2 n_e \hbar}{eH}\right)}{R_H^2} \langle \delta n V_{ac} \cos(2\pi ft) \rangle.$$

By injecting in this formula the expression of δn as a function of V_{ac} , and using the relation $V_{PV} = i_{dc} R_H$ with the ap-

proximation $R_H = H/(en_e)$ that is accurate below 1 T, we obtain

$$V_{PV} \approx \frac{eC}{\hbar} R_1(H) \sin\left(\frac{2\pi^2 n_e \hbar}{eH}\right) V_{ac}^2. \quad (2)$$

In this expression $R_1(H)$ is the typical SdH oscillation amplitude that is symmetric with magnetic field. Consequently this expression reproduces the main features observed in our experiment. V_{PV} is antisymmetric with magnetic field, with a phase given by $\sin(\frac{2\pi^2 n_e \hbar}{eH})$ and an amplitude that scales proportionally to microwave power $V_{PV} \propto V_{ac}^2 \propto P$. This expression also leads to the right order of magnitude for the observed photovoltaic voltage, indeed, for $C \approx \epsilon_0 D$ with $D \approx 1 \mu\text{m}$, $V_{ac}^2 = 1 \text{ nW} \times 50 \Omega$ and $R_1(H) \approx 1 \text{ k}\Omega$ at $H \approx 1 \text{ T}$, we find that $V_{PV} \approx 0.1 \mu\text{V}$ (experimental amplitude is shown in the right panel of Fig. 2). Further comparison is possible by noting that the product $R_1(H) \sin(\frac{2\pi^2 n_e \hbar}{eH})$ is proportional to $dR_{xx}(H^{-1})/dH^{-1}$. In our approximation, this leads to the simple prediction

$$\int V_{PV}(H^{-1}) dH^{-1} \propto R_{xx}(H^{-1}). \quad (3)$$

In Fig. 5, we show that this relation is well verified as long as $H^{-1} \geq 1.5 \text{ T}^{-1}$. Deviations are observed for higher magnetic fields, specially at $H^{-1} \approx 0.5 \text{ T}^{-1}$ where a plateau appears in V_{PV} that is not present in R_{xx} . We attribute this deviation to other quantum effects which are not taken into account in our simple model and become relevant at higher magnetic field. Specially the physics of the quantum-Hall effect is important, while our model is based on a Shubnikov–de Haas approximation for conductivity.

We have also measured the temperature dependence of photovoltaic effect. Our results summarized in Fig. 6 show that the amplitude of the photovoltaic oscillations strongly decreases with temperature in the 100 mK–1 K range, in a similar way to SdH oscillations on the linear resistance. To achieve a more quantitative comparison we have tried to extract the carrier effective mass from the temperature dependence of the amplitude of the SdH oscillations of the photovoltage. As shown in Fig. 5 this dependence is well described by a relation of the form

$$\ln \frac{|V_{PV}|}{T} = -A \frac{T}{B} + \text{const.} \quad (4)$$

For SdH oscillations of the resistivity the coefficient A is equal to $A_0 = \frac{2\pi^2 k_B m^*}{e\hbar}$. In the case of photovoltage oscillations of resistivity, we find a higher value $A \approx 3.5A_0$. While de-

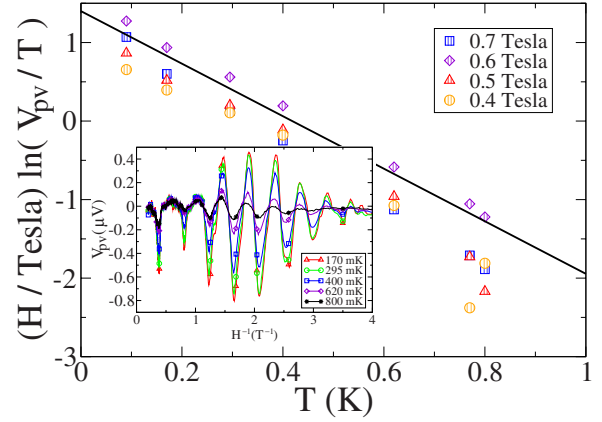


FIG. 6. (Color online) Dependence of the photovoltage on temperature for several magnetic fields in semilogarithmic scale. The data for different magnetic fields can be rescaled on a single linear curve as predicted by Eq. (4). The inset shows the photovoltage dependence on inverse magnetic fields for different temperatures for $f=2.5 \text{ GHz}$ and $P=1 \text{ nW}$.

tailed studies as a function of both temperature and microwave power are needed to establish the origin of this discrepancy, this most likely indicates that there is an additional energy scale in the problem which is related to microwave power.

V. CONCLUSIONS

In conclusion we have investigated the photovoltaic effect in high-mobility two dimensional electron gas under irradiation by an evanescent microwave potential. We have found that the photovoltaic voltage exhibits zero centered oscillations as a function of inverse magnetic field. These oscillations are antisymmetric with magnetic field and are out of phase with the well-known Shubnikov-de Haas oscillations in resistivity as a function of inverse magnetic field. The amplitude of these oscillations is proportional to microwave power. Our experimental findings can be understood from a simple model that predicts the creation of stationary orbital currents in the sample under microwave driving. In this model the stationary voltage across the sample appears as a Hall-effect detection of the orbital currents.

ACKNOWLEDGMENTS

We are grateful to J. Gabelli, B. Reulet, M. Ferrier, R. Deblock, and U. Gennser for stimulating discussions, and we acknowledge ANR NANOTERA and DGA for support.

¹B. L. Altshuler and D. E. Khmel'nitskii, JETP Lett. **42**, 359 (1985); A. I. Larkin and D. E. Khmel'nitskii, Sov. Phys. JETP **64**, 1075 (1986).

²V. Fal'ko and D. Khmel'niskii, Zh. Eksp. Teor. Fiz. **95**, 328 (1989) [Sov. Phys. JETP **68**, 186 (1989)].

³R. A. Webb, S. Washburn, and C. P. Umbach, Phys. Rev. B **37**, 8455 (1988); P. G. N. de Vegvar, G. Timp, P. M. Mankiewich, J. E. Cunningham, R. Behringer, and R. E. Howard, *ibid.* **38**, 4326 (1988).

⁴A. Bykov, G. Gusev, and Z. Kvon, Zh. Eksp. Teor. Fiz. Pis'ma

- Red. **49**, 13 (1989) [JETP Lett. **49**, 13 (1989)].
- ⁵S. Washburn and R. A. Webb, *Adv. Phys.* **35**, 375 (1986).
- ⁶M. Büttiker, *Phys. Rev. Lett.* **57**, 1761 (1986).
- ⁷D. Sanchez and M. Büttiker, *Phys. Rev. Lett.* **93**, 106802 (2004).
- ⁸R. E. Bartolo, N. Giordano, X. Huang, and G. H. Bernstein, *Phys. Rev. B* **55**, 2384 (1997).
- ⁹L. DiCarlo, C. M. Marcus, and J. S. Harris, *Phys. Rev. Lett.* **91**, 246804 (2003).
- ¹⁰L. Angers, A. Chepelianski, R. Deblock, B. Reulet, and H. Bouchiat, *Phys. Rev. B* **76**, 075331 (2007).
- ¹¹J. Wei, M. Shimogawa, Z. Wang, I. Radu, R. Dormaier, and D. H. Cobden, *Phys. Rev. Lett.* **95**, 256601 (2005).
- ¹²R. Leturcq, D. Sanchez, G. Gotz, T. Ihn, K. Ensslin, D. C. Driscoll, and A. C. Gossard, *Phys. Rev. Lett.* **96**, 126801 (2006).
- ¹³D. M. Zumbuhl, C. M. Marcus, M. P. Hanson, and A. C. Gossard, *Phys. Rev. Lett.* **96**, 206802 (2006).
- ¹⁴L. Angers, E. Zarka-Bajjani, R. Deblock, S. Gueron, H. Bouchiat, A. Cavanna, U. Gennser, and M. Polianski, *Phys. Rev. B* **75**, 115309 (2007).
- ¹⁵B. Spivak, F. Zhou, and M. T. Beal Monod, *Phys. Rev. B* **51**, 13226 (1995).
- ¹⁶M. Moskalets and M. Büttiker, *Phys. Rev. B* **69**, 205316 (2004).
- ¹⁷S. Sassine, Y. Krupko, J. C. Portal, Z. D. Kvon, R. Murali, K. P. Martin, G. Hill, and A. D. Wieck, *Phys. Rev. B* **78**, 045431 (2008).
- ¹⁸A. D. Chepelianskii, M. V. Entin, L. I. Magarill, and D. L. Shepelyansky, *Eur. Phys. J. B* **56**, 323 (2007).
- ¹⁹J. Q. Zhang, S. Vitkalov, Z. D. Kvon, J. C. Portal, and A. Wieck, *Phys. Rev. Lett.* **97**, 226807 (2006).
- ²⁰K. v. Klitzing, G. Dorda, and M. Pepper, *Phys. Rev. Lett.* **45**, 494 (1980).
- ²¹D. Shoenberg, *Magnetic Oscillations in Metals* (Cambridge University Press, Cambridge, UK, 1984).
- ²²We notice that the symmetry is broken by the presence of an oval dot between the left [*S*] and [*C*] gates; this weak asymmetry does not play a role for the effect discussed in this paper but is analyzed more carefully in A. D. Chepelianskii and H. Bouchiat, *Phys. Rev. Lett.* **102**, 086810 (2009).
- ²³A. A. Bykov, *JETP Lett.* **87**, 233 (2008).
- ²⁴M. A. Zudov, R. R. Du, J. A. Simmons, and J. R. Reno, *Phys. Rev. B* **64**, 201311(R) (2001).
- ²⁵R. G. Mani, J. H. Smet, K. von Klitzing, V. Narayanamurti, W. B. Johnson, and V. Umansky, *Nature (London)* **420**, 646 (2002).
- ²⁶M. A. Zudov, R. R. Du, L. N. Pfeiffer, and K. W. West, *Phys. Rev. Lett.* **90**, 046807 (2003).